Quantum Chemical Interaction Energy Surfaces of Ethylene and Propene Dimers

Jukka-Pekka Jalkanen, Sallaraisa Pulkkinen, and Tapani A. Pakkanen*

Department of Chemistry, University of Joensuu, PO Box 111, FIN-80101 Joensuu, Finland

Richard L. Rowley

Department of Chemical Engineering, Brigham Young University, Provo, Utah 84602

Received: June 19, 2004; In Final Form: January 30, 2005

Ab initio studies of nonbonding interactions for ethylene and propene dimers were conducted at the MP2/6-311+G(2df,2pd) level. The dimers were attractive in all of the orientations studied; however, the attraction was <0.1 kcal/mol for ethylene D_{2h} and C_{2h} dimers, for which the π-electron clouds or H atoms interact closely. A previously introduced transferable potential model, NIPE [Jalkanen, J.-P.; Pakkanen, T. A.; Yang, Y.; Rowley, R. L. *J. Chem. Phys.* **2003**, *118*, 5474], which is based on quantum chemical calculations of small alkane molecules, was tested against the propene and ethylene dimer data. Comparisons of results showed that interaction energies for orientations dominated by interactions between the propene methyl groups or two hydrogens were accurately predicted with the NIPE model. Interactions involving the double bond were not predicted as well, because the original NIPE regression data set did not contain any information about π-electron systems. An extension of the NIPE model to include π-electron interactions is proposed. Additional interaction sites are used with the same energy function as atomic interactions. This addition provides a more accurate description of the interaction energies of both ethylene and propene and extends the transferability of the NIPE model to alkenes.

1. Introduction

Alkanes and noble gases offer a good starting point in understanding the nonbonding interactions of molecules. They do not have polar groups masking the weaker van der Waals forces with stronger charge−charge interactions. Our previous work concentrated on studying the interaction energy surfaces of saturated hydrocarbons with ab initio methods. This model was termed NIPE, as an acronym formed from the first letters of neopentane, isobutane, propane, and ethane. Ab initio nonbonding energy data for these molecules were used in the construction of NIPE. These energy surfaces were then fitted with a transferable, pairwise-additive potential that was based on a simple potential energy function between pairs of atoms. To the extent that such site−site or interatomic interaction models are transferable, when used in conjunction with molecular dynamics simulations, they provide a powerful tool for predictive calculations of fluid properties and phenomena. It was recently shown that this approach can be applied effectively with good transferability to some strained cyclic alkanes,[1] in addition to small and branched alkanes from which the method was developed. The next logical test of the NIPE hydrocarbon potential model is the unsaturated hydrocarbons. The description of hydrocarbon π-electron systems is challenging, because they introduce many special features, such as CH−π interactions, conjugated effects, and aromaticity.

In the past few years, several theoretical studies have been published concerning the nonbonding behavior of π-electron systems. Even in the case of the simplest alkene, ethylene, there are new contributions to the interaction energy that are not typically found between alkanes, although some interactions of strained cyclic structures resembling π-systems have been reported.[2,3] A transferable way of describing these interactions is required if reliable results are desired for interaction energies between larger molecules containing double-bonded atoms. The nonbonding interactions of ethylene dimers have been a popular subject for ab initio studies, because of ethylene's small size and simplicity.[4−9] Theoretical studies of propene dimer interaction energies, on the other hand, are less common. Both are systems for which comparisons can be made to alkane potential energy surfaces, and the differences can be identified as arising from the effects of the sp^2 hybridized C atoms. More-complicated phenomena, such as conjugated effects and aromaticity, do not need to be considered in the study of these molecules.

Interaction studies of various hydrocarbon systems[6−26] have provided valuable insight on the computational methods needed to capture electron correlation effects, which are essential for description of dispersion forces. The suggested origin of CH−π interactions has been charge transfer (see, for example, ref 27 and references therein); however, more-recent higher-level theoretical studies of benzene/ethylene and ethylene/methane concluded that a major contribution to CH−π intermolecular attraction results from dispersion forces.[12,20,21,28] Generally, the $\pi-\pi$ interaction is considered repulsive, because the two π-electron clouds repel each other. Hunter and Sanders[29] used this assumption when studying the origins of aromatic π-stacking. They suggested a simple model that described both CH−π and $\pi-\pi$ interactions with partial charges, attributing these effects entirely to Coulombic interactions.

This work has been concentrated on studying the intermolecular potential energy surface of ethylene and propene dimers. These are two of the simplest alkenes, and propene, in particular, is an interesting subject for study, because it combines a π-electron system with a saturated methyl group in the same

10.1021/jp047325c CCC: $30.25
Published on Web 03/08/2005

molecule. This type of molecule serves as a link between saturated and unsaturated systems and can be used to regress model interaction parameters between the two types of systems. In this paper, we will show that the previously published NIPE potential model can be applied to interactions between the saturated carbon of propene with good accuracy, but an isotropic, spherical, atom-centered model may not be the best way to describe the π-electron effects. Instead, we propose a simple addition of interaction sites, representing the high electron density of the double bond, as a convenient way to improve the accuracy of the parametrized energy surface descriptions of ethylene and propene dimers.

2. Computational Details

Inclusion of electron correlation effects with Møller−Plesset perturbation theory (MP*n*) has previously been found suitable for description of nonbonding effects of saturated alkanes if combined with sufficiently large basis sets.[4,5,8−12,28,30−32] In these cases, the second-order perturbation treatment (MP2) does not appreciably differ from results obtained with MP4(SDTQ) or CCSD(T) methods.[5,8,11,28,31,33] However, the presence of a double bond may alter the situation. MP2 results for some aromatic molecules have shown that intermolecular attraction was overestimated by ∼20%−30%, because of missing triple excitations.[7,9,15,16,22,24,30] In this work, both ethylene and propene monomers were optimized at the MP2/6-311+G(2df,2pd) level, using Gaussian98.[34] The selected basis set was previously shown to capture ∼85% of the total interaction energy of the propane dimer at the complete basis set limit.[30] The errors that result from the selection of an incomplete basis set and second-order perturbation treatment for electron correlation are of opposite signs. The interaction energy of the ethylene D_{2d} dimer[5] with CCSD(T)/cc-PVQZ(-g,f) is −1.29 kcal/mol, which is in pretty good agreement with the value that we obtain from MP2/6-311+G(2df,2pd) calculations (−1.199 kcal/mol for the same dimer orientation). This agreement is slightly better than that obtained with the propane dimer.[30] Šponer and Hobza reported similar observations for formamide[16] dimers: MP2 calculations with an adequate basis set produced results that were very similar to CCSD(T) computations for the methane−ethylene system. This agreement is somewhat fortuitous; however, it seems that counterpoise-corrected[35] ab initio results using MP2/6-311+G(2df,2pd) should provide a reasonable estimate of the nonbonding behavior of ethylene and propene dimers. The MP2/6-311+G(2df,2pd) optimized structures were kept fixed and used throughout this study. Also, all supermolecule calculations were conducted at this level. Optimized bond lengths, bond angles, and dihedral angles are given in Table 1. Table 2 summarizes the ethylene D_{2d} results calculated at various levels of electron correlation, reported on some previous studies. The ethylene results[9,24,28] for the interaction energy obtained from MP2 calculations with a suitably large basis set were similar to those obtained with higher-quality electron correlation methods.

3. Interaction Energy Surfaces

A complete description of the total six-dimensional space that describes all possible relative orientations of the two molecules would require a substantial amount of computation. We have simplified the description of relative orientations by considering each molecule to consist of vertexes, edges, and faces, which are defined by the outermost hydrogen nuclei in each molecule. Hence, ethylene consists of one hydrogen vertex (*a*) and two edges (*aa* short, which is defined as that between H atoms attached to the same carbon, and *aa* long, which is defined as that between H atoms attached to adjacent carbons). The *aaaa*-face is in the plane of the atoms. The propene geometry is more complicated, because it consists of five different vertexes (*a, b, c, d,* and *e*), eight edges (*aa, ab, ac, ad, ae, bc, be,* and *de*), and five faces (*aac, aad, abc, abe,* and *ade*). These are illustrated in Figure 1. The intermolecular approach axis between the two molecules is defined by the different combinations of faces, edges, and vertexes of both monomers.

TABLE 1: Ethylene and Propene Structural Parameters

parameter	value
Ethylene	
bond length	
r(C−C)	1.3316 Å
r(C−Ha)	1.0804 Å
bond angle, a(H−C−C)	121.3597°
dihedral angle, d(H−C−C−H)	±180.°
point group	D_{2h}
Propene	
bond lengths	
r(C2−C1)	1.3337 Å
r(C3−C1)	1.5039 Å
r(Hd−C2)	1.0811 Å
r(He−C2)	1.0811 Å
r(Hb−C1)	1.0832 Å
r(Ha−C3)	1.0890 Å
r(Hc−C3)	1.0890 Å
bond angles	
a(Hd−C2−C1)	121.2986°
a(He−C2−C1)	121.2986°
a(Hb−C1−C2)	118.2809°
a(Ha−C3−C1)	111.1065°
a(Hc−C3−C1)	111.5737°
dihedral angles	
d(Hd−C2−C1−He)	180.°
d(Hb−C1−C2−He)	0.°
d(Hc−C3−C1−Hb)	0.°
d(Ha−C3−C1−C2)	±59.8207°
point group	C_s

TABLE 2: Comparison of Ethylene D_{2d} Dimer Interaction Energies Calculated with Various Methods and Basis Sets

method	E_{min} (kcal/mol)	reference
MP2/aug(d,p)-6-311G**	−1.230	Tsuzuki et al.[28]
MP3/aug(d,p)-6-311G**	−1.105	Tsuzuki et al.[28]
MP4(SDQ)/aug(d,p)-6-311G**	−0.928	Tsuzuki et al.[28]
MP4(SDTQ)/aug(d,p)-6-311G**	−1.192	Tsuzuki et al.[28]
CCSD/aug(d,p)-6-311G**	−0.897	Tsuzuki et al.[28]
CCSD(T)/aug(d,p)-6-311G**	−1.150	Tsuzuki et al.[28]
CCSD(T)/cc-pVQZ(-g,f)	−1.29	Tsuzuki et al.[24]
MP2/6-311+G(2df,2pd)	−1.199	present work

The distance between the monomers along the approach axis varies, as measured from the centerpoint of the π-bond for ethylene and from the nucleus of the C1 carbon for propene. The combination of each of the vertexes, edges, and faces of monomer A with similar constructs in monomer B results in 10 relative orientations for ethylene and 171 combinations for propene dimers. The six archetypes of orientations (combinations of faces, edges, and vertexes) are illustrated in Figure 2. These orientations are referenced as routes throughout this paper.

Ten additional ethylene routes were investigated, where one of the dimers was rotated from 0° to 90° about the approach axis (for example, ethylene *aal-aal* 0 and *aal-aal* 90). The latter is also illustrated on the left side of Figure 3. Energies were calculated at ∼13 different distances along each route, to sample the potential hypersurface; this action resulted in 2289 propene and 276 ethylene dimer data points for the routes mentioned previously.

A. Ethylene. All ethylene dimer orientations show attraction, albeit the energy minima for the *a*−*a* and *aaaa*−*aaaa* routes

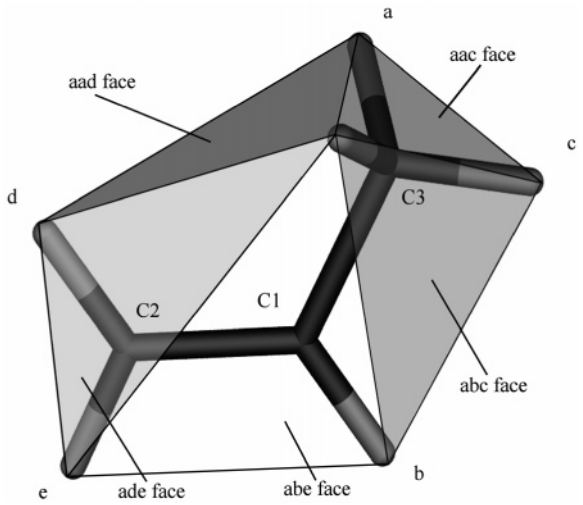

Figure 1. Propene atom labels. Different vertexes are labeled as *a* through *e*. Edges and faces are named after the vertexes. Faces consist of the three outermost hydrogens.

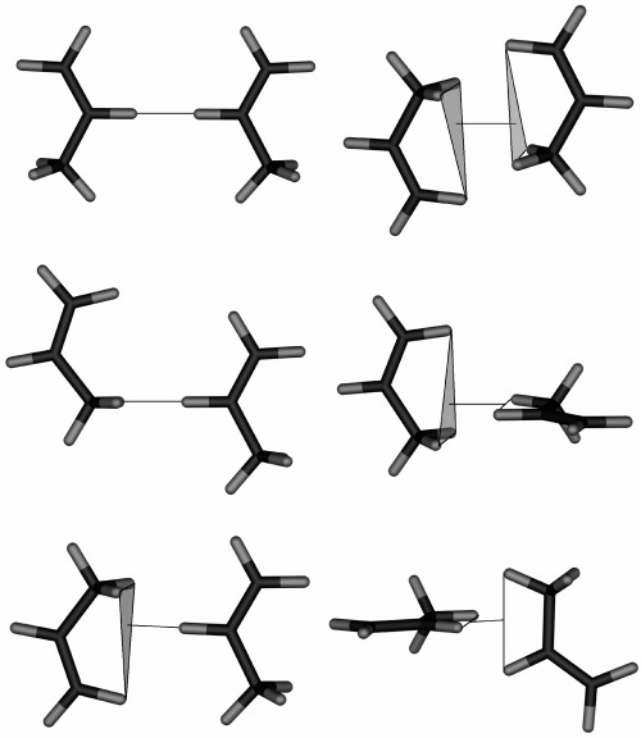

Figure 2. Six archetypes of propene orientations. Starting from top left-hand corner and proceeding anticlockwise: vertex−vertex (*b*−*b*), vertex−edge (*b*−*aa*), vertex−face (*b*−*aad*), edge−edge (*bc*−*bc*), edge−face (*bc*−*aad*), and face−face (*aad*−*aad*). The actual route name is given in parentheses for each of the shown cases. The propene molecule consists of five vertexes, eight edges, and five faces, resulting in 171 different combinations of these moieties. The solid line between the propene molecules illustrates the intermolecular approach axis. The intermolecular distance is always reported as a separation of centermost carbon (C1) atoms. The intermolecular approach axis is perpendicular to any face or edge. Whenever vertexes are concerned, the approach axis goes along the C−H bond.

are very shallow (between 0 and −0.1 kcal/mol). The energies for these two routes vary only slightly with the rotation about the intermolecular approach axis. Counterpoise-corrected energies, as a function of distance for each route or relative orientation, were fitted to the equation

$$E = -\epsilon\{1 - [1 - e^{-A(r-r^*)}]^2\} \quad (1)$$

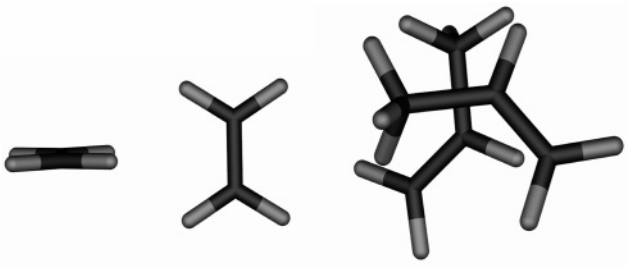

Figure 3. The most favorable orientation of the ethene D_{2d} dimer, *aal*−*aal* 90 route (top) and propene, *ab*−*ab* 90 route (bottom). Energy minimum of −1.199 kcal/mol was observed with the ethene dimer and −1.765 kcal/mol with the propene dimer at the MP2/6-311+G(2df,-2pd) level.

TABLE 3: Parameters for Ethylene MP2/6-311+G(2df,2pd) Interaction Energy Curves

orientation[a]	ϵ (kcal/mol)	A (Å^{-1})	r^* (Å)	SSR
a−*a* 0	0.090	1.722	5.688	0.000
a−*aas* 0	0.247	1.619	5.305	0.000
a−*aal* 0	0.350	1.590	4.601	0.000
a−*aaaa* 0	0.686	1.354	4.528	0.005
aas−*aas* 0	0.284	1.618	5.339	0.001
aas−*aal* 0	0.294	1.647	4.851	0.000
aas−*aaaa* 0	0.566	1.357	4.607	0.004
aal−*aal* 0	0.261	1.682	4.514	0.001
aal−*aaaa* 0	0.945	1.375	3.882	0.008
aaaa−*aaaa* 0	0.037	1.559	4.689	0.001
a−*a* 90	0.131	1.648	5.565	0.001
a−*aas* 90	0.329	1.572	5.259	0.001
a−*aal* 90	0.502	1.536	4.542	0.001
a−*aaaa* 90	0.691	1.356	4.524	0.005
aas−*aas* 90	0.529	1.540	5.088	0.003
aas−*aal* 90	0.816	1.511	4.394	0.003
aas−*aaaa* 90	0.548	1.347	4.613	0.005
aal−*aal* 90	1.199	1.490	3.777	0.003
aal−*aaaa* 90	0.920	1.347	3.854	0.006
aaaa−*aaaa* 90	0.031	1.553	4.713	0.001

[a] Numbers in route names identify the intermolecular rotation angle (in degrees).

to simplify the presentation of the large amount of numerical data. The parameters A, ϵ, and r^* obtained are given in Table 3, along with the sum of squared residuals (SSR) of the fit (given in units of (kcal/mol)^2 per route). As the parameters in Table 3 indicate, rotation from ethylene *aaaa*−*aaaa* 0 (D_{2h}) to *aaaa*−*aaaa* 90 (D_{2d}) degrees has only negligible impact on the interaction energy; i.e., the energy surface is relatively flat and ϵ changes only slightly. However, a large change in energy is observed when *aal*−*aal* 0 is rotated 90°, from −0.26 kcal/mol to −1.20 kcal/mol. In this case, the π-electron clouds rotate from a parallel orientation to the more-favorable perpendicular orientation.

B. Propene. The propene molecule consists of a methyl group, in addition to the π-electron double bond environment found in ethylene. Intermolecular rotation angles for propene dimers were selected based on chemical intuition, to avoid head-on approaches between atoms as much as possible. Propene interaction energies were fitted with eq 1 in a manner similar to that used for ethylene. Parameters for interaction energy curves for propene are given in Table 4.

Based on the values of Table 4, an energy landscape can be constructed for propene dimer orientations (see Figure 4). This energy map can be used to determine favorable propene dimer orientations. Although not sufficiently detailed to determine the global minimum, the energy landscape obtained for the propene dimer orientations offers considerable insight into the nature

TABLE 4: Parameters for Propene MP2/6-311+G(2df,2pd) Interaction Energy Curves

orientation	ϵ (kcal/mol)	A (Å^{-1})	r^* (Å)	SSR	orientation	ϵ (kcal/mol)	A (Å^{-1})	r^* (Å)	SSR	orientation	ϵ (kcal/mol)	A (Å^{-1})	r^* (Å)	SSR
a−*a*	0.334	1.636	6.398	0.004	*d*−*ae*	0.991	1.435	5.106	0.011	*ac*−*abe*	0.695	1.421	4.996	0.007
a−−*b*	0.379	1.577	5.329	0.006	*d*−*bc*	0.626	1.422	4.946	0.002	*ac*−*ade*	0.701	1.379	5.230	0.007
a−*c*	0.276	1.689	6.436	0.003	*d*−*be*	0.645	1.562	5.208	0.005	*ad*−*ad*	1.376	1.346	4.858	0.009
a−*d*	0.461	1.483	5.808	0.008	*d*−*de*	0.443	1.526	6.310	0.002	*ad*−*ae*	1.322	1.425	4.533	0.016
a−*e*	0.294	1.543	5.892	0.004	*d*−*aac*	0.538	1.547	6.340	0.003	*ad*−*bc*	0.679	1.487	4.901	0.006
a−*aa*	0.667	1.444	5.635	0.006	*d*−*aad*	0.656	1.423	5.808	0.001	*ad*−*be*	1.470	1.367	4.163	0.008
a−*ab*	1.017	1.466	4.686	0.017	*d*−*abc*	1.015	1.432	4.759	0.011	*ad*−*de*	1.022	1.374	5.473	0.005
a−*ac*	0.413	1.510	5.743	0.002	*d*−*abe*	0.937	1.377	4.860	0.009	*ad*−*aac*	0.730	1.468	5.841	0.005
a−*ad*	0.563	1.376	5.596	0.001	*d*−*ade*	0.982	1.314	5.021	0.008	*ad*−*aad*	0.997	1.333	5.119	0.004
a−*ae*	0.913	1.492	5.021	0.005	*e*−*e*	0.155	1.713	6.584	0.001	*ad*−*abc*	1.422	1.419	4.257	0.012
a−*bc*	0.582	1.526	5.037	0.004	*e*−*aa*	0.426	1.628	6.319	0.003	*ad*−*abe*	1.034	1.397	4.412	0.006
a−*be*	0.589	1.559	4.984	0.004	*e*−*ab*	0.785	1.425	4.805	0.006	*ad*−*ade*	1.152	1.362	4.680	0.009
a−*de*	0.405	1.550	6.239	0.002	*e*−*ac*	0.413	1.509	5.879	0.002	*ae*−*ae*	0.696	1.511	4.142	0.000
a-−*aac*	0.538	1.517	6.259	0.003	*e*−*ad*	0.665	1.423	5.575	0.002	*ae*−*bc*	1.160	1.341	4.101	0.011
a−*aad*	0.595	1.405	5.654	0.002	*e*−*ae*	0.888	1.378	4.822	0.002	*ae*−*be*	1.043	1.449	4.220	0.008
a−*abc*	0.909	1.551	4.892	0.019	*e*−*bc*	0.529	1.516	5.122	0.002	*ae*−*de*	0.685	1.390	5.341	0.003
a−*abe*	0.984	1.370	4.694	0.008	*e*−*be*	0.470	1.511	4.924	0.001	*ae*−*aac*	0.725	1.412	5.421	0.006
a−*ade*	0.890	1.494	5.352	0.014	*e*−*de*	0.334	1.563	6.350	0.001	*ae*−*aad*	1.168	1.318	4.670	0.010
b−*b*	0.244	1.544	4.688	0.001	*e*−*aac*	0.445	1.565	6.366	0.002	*ae*−*abc*	1.478	1.411	3.716	0.013
b−*c*	0.244	1.605	5.437	0.001	*e*−*aad*	0.543	1.452	5.815	0.001	*ae*−*abe*	0.495	1.475	4.063	0.000
b−*d*	0.294	1.574	5.464	0.002	*e*−*abc*	0.648	1.523	4.853	0.004	*ae*−*ade*	0.846	1.432	4.084	0.001
b−*e*	0.207	1.608	5.538	0.002	*e*−*abe*	0.836	1.395	4.818	0.005	*bc*−*bc*	1.120	1.454	3.943	0.003
b−*aa*	0.500	1.529	5.277	0.003	*e*−*ade*	0.763	1.486	5.474	0.005	*bc*−*be*	1.234	1.475	3.946	0.006
b−*ab*	0.853	1.430	3.972	0.005	*aa*−*aa*	0.541	1.481	6.078	0.003	*bc*−*de*	0.906	1.319	5.228	0.012
b−*ac*	0.452	1.541	5.303	0.003	*aa*−*ab*	1.087	1.537	4.879	0.015	*bc*−*aac*	0.653	1.547	5.497	0.004
b−*ad*	0.741	1.574	4.684	0.098	*aa*−*ac*	0.490	1.513	6.085	0.002	*bc*−*aad*	0.767	1.427	4.895	0.003
b−*ae*	1.017	1.359	4.196	0.007	*aa*−*ad*	0.927	1.402	5.407	0.003	*bc*−*abc*	1.246	1.444	4.136	0.087
b−*bc*	0.538	1.496	4.276	0.001	*aa*−*ae*	0.791	1.328	4.990	0.007	*bc*−*abe*	1.228	1.333	3.917	0.014
b−*be*	0.566	1.514	4.217	0.002	*aa*−*bc*	0.800	1.426	4.851	0.002	*bc*−*ade*	1.051	1.413	4.503	0.017
b−*de*	0.401	1.512	5.519	0.002	*aa*−*be*	0.889	1.451	4.799	0.004	*be*−*be*	1.359	1.488	3.940	0.008
b−*aac*	0.511	1.530	5.538	0.003	*aa*−*de*	0.553	1.510	6.236	0.003	*be*−*de*	0.947	1.476	5.120	0.005
b−*aad*	0.635	1.395	4.897	0.002	*aa*−*aac*	0.549	1.557	6.378	0.004	*be*−*aac*	0.669	1.533	5.476	0.005
b−*abc*	0.938	1.448	4.069	0.011	*aa*−*aad*	0.626	1.429	5.768	0.003	*be*−*aad*	0.838	1.439	4.849	0.005
b−*abe*	0.960	1.341	4.016	0.009	*aa*−*abc*	0.992	1.442	4.684	0.008	*be*−*abc*	1.077	1.575	4.110	0.010
b−*ade*	0.916	1.411	4.381	0.008	*aa*−*abe*	0.799	1.397	5.030	0.010	*be*−*abe*	1.118	1.407	3.905	0.008
c−*c*	0.217	1.780	6.470	0.001	*aa*−*ade*	0.732	1.458	5.475	0.010	*be*−*ade*	1.023	1.493	4.507	0.009
c−*d*	0.250	1.697	6.473	0.002	*ab*−*ab*	1.730	1.517	3.505	0.022	*de*−*de*	0.629	1.486	6.403	0.004
c−*e*	0.253	1.534	6.080	0.002	*ab*−*ac*	1.015	1.455	4.894	0.013	*de*−*aac*	0.524	1.537	6.611	0.003
c−*aa*	0.440	1.507	5.744	0.003	*ab*−*ad*	1.471	1.381	4.054	0.007	*de*−*aad*	0.626	1.419	6.018	0.003
c−*ab*	0.791	1.436	4.905	0.008	*ab*−*ae*	1.157	1.572	3.906	0.005	*de*−*abc*	0.775	1.534	5.181	0.006
c−*ac*	0.394	1.500	5.784	0.002	*ab*−*bc*	1.389	1.428	3.754	0.016	*de*-*abe*	0.680	1.387	5.166	0.004
c−*ad*	0.537	1.393	5.683	0.001	*ab*−*be*	1.233	1.491	3.822	0.011	*de*−*ade*	0.625	1.426	5.568	0.003
c−*ae*	0.860	1.467	5.182	0.012	*ab*−*de*	0.932	1.433	5.002	0.006	*aac*−*aac*	0.523	1.562	6.722	0.002
c−*bc*	0.488	1.491	4.870	0.001	*ab*−*aac*	0.844	1.443	5.141	0.007	*aac*−*aad*	0.656	1.483	6.126	0.002
c−*be*	0.548	1.641	5.191	0.003	*ab*−*aad*	0.962	1.392	4.711	0.011	*aac*−*abc*	0.906	1.544	5.240	0.007
c−*de*	0.378	1.582	6.066	0.001	*ab*−*abc*	1.473	1.534	3.737	0.021	*aac*−*abe*	0.737	1.401	5.249	0.007
c−*aac*	0.447	1.564	6.305	0.001	*ab*−*abe*	0.968	1.486	3.705	0.002	*aac*−*ade*	0.697	1.442	5.648	0.005
c−*aad*	0.549	1.466	5.777	0.001	*ab*−*ade*	0.762	1.448	4.043	0.001	*aad*−*aad*	0.899	1.391	5.521	0.004
c−*abc*	0.718	1.555	4.812	0.007	*ac*−*ac*	0.443	1.539	6.096	0.002	*aad*−*abc*	1.109	1.475	4.787	0.009
c−*abe*	0.859	1.400	4.873	0.010	*ac*−*ad*	0.645	1.426	5.421	0.001	*aad*−*abe*	1.032	1.329	4.643	0.012
c−*ade*	0.750	1.468	5.300	0.009	*ac*−*ae*	0.682	1.353	5.058	0.006	*aad*−*ade*	0.859	1.401	5.184	0.011
d−*d*	0.289	1.577	6.507	0.003	*ac*−*bc*	0.608	1.508	5.036	0.002	*abc*−*abc*	1.297	1.543	3.704	0.017
d−*e*	0.253	1.532	6.081	0.002	*ac*−*be*	0.787	1.483	4.898	0.006	*abc*−*abe*	1.173	1.532	3.865	0.006
d−*aa*	0.485	1.598	6.306	0.003	*ac*−*de*	0.468	1.599	6.283	0.013	*abc*−*ade*	1.182	1.590	4.349	0.010
d−*ab*	0.920	1.407	4.769	0.007	*ac*−*aac*	0.484	1.539	6.418	0.002	*abe*−*abe*	0.458	1.428	3.949	0.000
d−*ac*	0.459	1.622	6.310	0.003	*ac*−*aad*	0.582	1.424	5.749	0.002	*abe*−*ade*	0.827	1.438	4.073	0.001
d−*ad*	0.766	1.410	5.543	0.002	*ac*−*abc*	0.851	1.524	4.884	0.008	*ade*−*ade*	0.929	1.576	4.663	0.005

of the interactions, and it can be used as a starting point for further studies.

Figure 4 shows that the most attractive route for propene is the edge−edge route *ab*−*ab*, as illustrated on the right side of Figure 3. An energy minimum of −1.730 kcal/mol is observed at a C1 carbon separation of ∼3.5 Å. For comparison purposes, this attraction is significantly less than the interaction energy of propene with the Na^+ ion[36] (−18.4 kcal/mol). It seems that propene molecules favor this orientation over *be*−*be*, which is a similar orientation to that observed to be most favorable for ethylene dimers. The difference in energy between *ab*−*ab* and *be*−*be* routes is ∼0.4 kcal/mol. This is probably due to attraction between methyl groups and π-electron clouds. Generally, routes dominated by the direct exposure of the C sp^2−C sp^3 bond have the largest attractive energies. These orientations, along with the *ad*-edge routes, avoid direct contact of the π-electron clouds in both monomers. This observation is in accordance with previous results for various π-electron systems.[24,29] None of the propene route combinations used in this work contains the direct approach of the stacked π-electron clouds similar to ethylene D_{2h} dimer. As was found previously with small alkanes,[33,37−39] the vertex−vertex routes show only slight attraction. Usually, these orientations place most of the atoms in a molecule far away from each other, so that their contribution to the total interaction energy is small.

4. Fitting Ab Initio Results with Pair Potentials

A. NIPE Predictions of Alkene Data. The recently introduced NIPE model[39] for alkanes uses transferable, pairwise-

	a	b	c	d	e	aa	ab	ac	ad	ae	bc	be	de	aac	aad	abc	abe	ade
a	0.334	0.379	0.276	0.461	0.294	0.667	1.017	0.413	0.563	0.913	0.582	0.589	0.405	0.538	0.595	0.909	0.984	0.890
b		0.244	0.244	0.294	0.207	0.500	0.853	0.453	0.741	1.017	0.538	0.566	0.401	0.511	0.635	0.938	0.960	0.916
c			0.217	0.250	0.253	0.440	0.791	0.394	0.537	0.860	0.488	0.548	0.378	0.447	0.549	0.718	0.859	0.750
d				0.289	0.252	0.485	0.920	0.459	0.766	0.991	0.626	0.645	0.443	0.538	0.656	1.015	0.937	0.982
e					0.155	0.426	0.785	0.413	0.665	0.888	0.529	0.470	0.334	0.445	0.543	0.648	0.836	0.763
aa						0.540	1.087	0.490	0.927	0.791	0.800	0.889	0.553	0.549	0.626	0.993	0.799	0.732
ab							1.730	1.015	1.471	1.157	1.389	1.233	0.932	0.844	0.962	1.473	0.968	0.762
ac								0.443	0.645	0.682	0.608	0.787	0.468	0.484	0.582	0.851	0.695	0.701
ad									1.376	1.321	0.679	1.470	1.022	0.730	0.997	1.422	1.034	1.152
ae										0.696	1.160	1.043	0.685	0.725	1.168	1.478	0.495	0.846
bc											1.120	1.234	0.906	0.653	0.767	1.246	1.228	1.051
be												1.359	0.947	0.669	0.838	1.077	1.118	1.023
de													0.629	0.524	0.626	0.775	0.680	0.625
aac														0.523	0.656	0.906	0.737	0.697
aad															0.899	1.109	1.032	0.859
abc																1.298	1.173	1.182
abe																	0.458	0.827
ade																		0.929

Well depth (kcal mol^{-1})	<0.3	0.3-0.7	0.701-1.1	1.101-1.5	>1.5

Figure 4. Propene dimer well depths. White background indicates a shallow potential well, and black cells reflect the strongest attractive interaction. Numbers in cells show the well depth in units of kcal/mol.

additive, interatomic potentials to predict the intermolecular pair potential of more-complex molecules. The NIPE model was originally regressed based on ab initio data for neopentane, isobutane, propane, and ethane. Recall that the acronym NIPE comes from the first letters of these molecules. Because the NIPE model uses interatomic contributions, it is unclear how and if such contributions are affected by bond order and the associated difference in electron density distribution. To test the extensibility of the NIPE model to alkenes, we compare its predictions, without consideration of the double bond, directly to our ab initio results.

In the NIPE model, the total interaction energy between molecules is computed as a sum of pair interactions between nonbonded atoms on the two interacting molecules. Each atomic pair interaction is calculated using eq 1 and the NIPE parameters for A, ϵ, and r^* for all C−C, C−H, and H−H interactions. Possible contributions arising from dispersion, polarization, exchange−repulsion, etc., were included as a part of these total interaction parameters. The NIPE model did not use combining rules to describe the cross interactions between two different atom types. In fact, cross-interaction parameters were determined to be quite different than previously proposed combining rules. The cross C−H interaction was determined to be much more attractive than either of the like−like interactions. The NIPE parameters were determined to represent the entire energy landscape of pairs of small normal and branched alkanes accurately. It was also shown recently that NIPE models the interaction energies of some cyclic alkanes[1] with reasonable accuracy. The energy surfaces of some highly strained cycloalkanes were not described as well; however, cyclohexane dimer interactions were well-predicted by the NIPE. Because of its simplicity, NIPE can be easily used in molecular dynamics simulations, where a simple yet accurate potential model is preferred. The modified Morse function (eq 1) used in NIPE seems to model interactions between atoms in the sp^3 bonded environment quite well, as evidenced by the wide variety of intermolecular interactions that it accurately describes.[1,33,37−42] When the energy landscape predicted by the NIPE model was compared to the ab initio alkene data, two things were apparent.

First, routes directed toward the π-cloud electrons were poorly predicted with the original NIPE parameter set (see Figure 5). The top portion of Figure 5 shows the squared difference between NIPE and MP2/6-311+G(2df,2pd) energies (given in units of (kcal/mol)^2) per data point on each route. The white cell background represents cases where no significant difference between the two methods is observed. Larger errors are indicated with darker background shading, and the most severe errors have a black background. As can be seen from the top portion of Figure 5, most of the error is concentrated on routes that involve either an *ae*-edge or an *abe*-face. This is probably because the

	a	b	c	d	e	aa	ab	ac	ad	ae	bc	be	de	aac	aad	abc	abe	ade
a	0.032	0.039	0.021	0.015	0.038	0.007	0.019	0.003	0.069	0.341	0.020	0.048	0.002	0.034	0.024	0.011	0.228	0.063
b		0.007	0.014	0.006	0.013	0.004	0.005	0.007	0.272	0.173	0.039	0.117	0.005	0.122	0.003	0.018	0.211	0.015
c			0.016	0.009	0.010	0.009	0.154	0.006	0.020	0.454	0.026	0.091	1.222	0.028	0.010	0.005	0.264	0.133
d				0.006	0.010	0.006	0.043	0.007	0.012	0.419	0.017	0.071	0.002	0.095	0.031	0.004	0.337	0.048
e					0.018	0.008	0.047	0.017	0.015	0.246	0.051	0.128	0.008	0.102	0.004	0.003	0.250	0.022
aa						0.064	0.036	0.050	0.011	0.440	0.006	0.045	0.014	0.006	0.044	0.002	0.605	0.168
ab							0.418	0.017	0.005	0.520	0.060	0.055	0.025	0.026	0.280	0.043	0.087	0.052
ac								0.031	0.001	0.373	0.008	0.062	0.045	0.001	0.036	0.000	0.511	0.195
ad									0.213	0.025	0.026	0.022	0.016	0.004	0.003	0.023	0.118	0.138
ae										0.084	0.068	0.020	0.140	0.197	0.096	0.218	0.210	0.072
bc											0.232	0.141	0.094	0.042	0.004	0.117	0.029	0.008
be												0.176	0.224	0.053	0.015	0.050	0.004	0.009
de													0.031	0.018	0.007	0.025	0.144	0.031
aac														0.008	0.009	0.029	0.160	0.058
aad															0.003	0.003	0.360	0.509
abc																0.135	0.159	0.089
abe																	0.356	0.030
ade																		0.016

	a	b	c	d	e	aa	ab	ac	ad	ae	bc	be	de	aac	aad	abc	abe	ade
a	0.038	0.046	0.025	0.016	0.037	0.003	0.038	0.003	0.046	0.030	0.016	0.032	0.010	0.030	0.017	0.014	0.020	0.066
b		0.006	0.021	0.006	0.014	0.012	0.012	0.004	0.321	0.043	0.010	0.017	0.024	0.069	0.021	0.001	0.031	0.055
c			0.019	0.015	0.012	0.017	0.009	0.006	0.013	0.033	0.020	0.071	0.237	0.023	0.006	0.003	0.018	0.041
d				0.008	0.012	0.013	0.003	0.006	0.011	0.053	0.004	0.022	0.032	0.049	0.070	0.006	0.052	0.014
e					0.028	0.004	0.003	0.008	0.015	0.053	0.032	0.031	0.004	0.056	0.011	0.006	0.026	0.066
aa						0.070	0.039	0.052	0.001	0.172	0.003	0.007	0.055	0.013	0.080	0.008	0.218	0.037
ab							0.214	0.061	0.042	0.090	0.054	0.017	0.014	0.005	0.124	0.016	0.013	0.073
ac								0.031	0.005	0.093	0.006	0.024	0.051	0.001	0.061	0.005	0.087	0.019
ad									0.036	0.042	0.010	0.027	0.005	0.003	0.001	0.108	0.029	0.021
ae										0.022	0.017	0.005	0.074	0.044	0.041	0.075	0.038	0.025
bc											0.027	0.019	0.013	0.016	0.010	0.061	0.008	0.027
be												0.020	0.028	0.011	0.017	0.015	0.021	0.005
de													0.002	0.001	0.065	0.010	0.152	0.017
aac														0.006	0.026	0.070	0.052	0.015
aad															0.023	0.005	0.256	0.222
abc																0.082	0.049	0.033
abe																	0.119	0.013
ade																		0.028

SSR per data point (kcal mol^{-1})^2	<0.05	0.05-0.099	0.1-0.1499	0.15-0.199	>0.2

Figure 5. Propene dimer error between NIPE predictions and ab initio results (SSR given in units of (kcal/mol)^2 per data point). The top figure shows the squared difference between the predictions of the original isotropic NIPE model and MP2/6-311+G(2df,2pd) results. The bottom figure shows the SSR when the anisotropic NIPE model is applied to propene data.

sp^2 C atom shape deviates strongly from the commonly used spherical models. In this case, the highest occupied molecular orbital (HOMO) is a π-orbital, aligned perpendicular to the plane of atoms in the π-system. The large error associated with the *be*- and *de*-edge routes is probably due to NIPE's spherical treatment of the sp^2 carbon, which would be too large (repulsion starts too early), when viewed from the side. A side approach toward the sp^2 carbon should allow closer contact between atoms than a top approach. The spherical atom approximation in NIPE predicts energies that are too repulsive for routes where the sp^2 carbon is approached from the side. The opposite effect is observed for the ethylene route *aaaa*−*aaaa* (see Figure 6) and for propene routes directed toward an *abe*-face or an *ae*-edge. In these cases, the NIPE predictions are too attractive because the $\pi-\pi$ interactions are not completely accounted for in the spherical approximation.

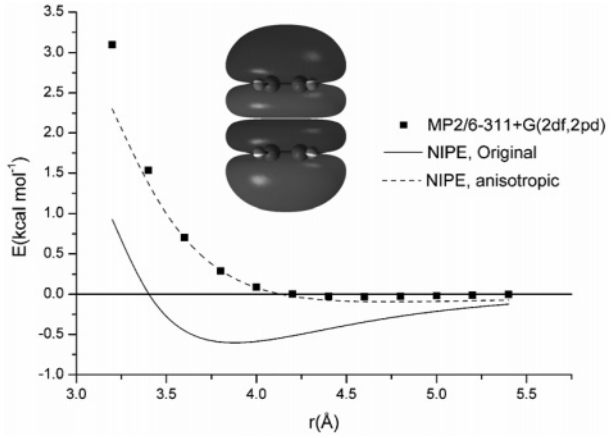

Figure 6. Ethylene *aaaa*−*aaaa* 0 route, according to MP2/6-311+G-(2df,2pd) results (denoted by solid squares, ■) and NIPE predictions (original NIPE denoted by a solid line (—), and anisotropic NIPE denoted by a dotted line (- - -)). The ethylene highest occupied molecular orbital (HOMO) is also shown. In this orientation, π-electron clouds are directly on top of each other, which makes interaction almost totally repulsive. The original NIPE model describes the interaction as attractive and allows a smaller distance between monomers.

The second observation concerns the vertex−vertex and methyl group interactions. NIPE energy predictions for these routes are in good agreement with the ab initio results. This suggests that NIPE parameters are transferable to saturated portion of the molecule, despite the presence of a π-system. The overall sum of squared residuals (SSR) when the original NIPE model was applied to the alkene systems was 0.101 (kcal/mol)^2 per data point. Half of that error came from <10% of the routes, and those were the routes that involved close contact between the π-systems. When the original NIPE model was applied to the propene data, 43 of 171 routes produced an SSR of >0.1 (kcal/mol)^2 per data point.

B. Improving the Performance of NIPE for Simple Alkenes. We attempted different approaches to improve the accuracy of the NIPE model in describing the nonbonding effects of ethylene and propene while preserving its transferability to alkyl groups. The error map for propene (see top portion of Figure 5) indicates that vertex−vertex and methyl group routes are well-described by NIPE parameters and they can be retained without sacrificing the accuracy of the fit. We constrained the propene methyl group parameters to NIPE values and optimized all other carbon, hydrogen, and cross-interaction parameters; however, results still showed significant error, with an SSR value of 0.085 (kcal/mol)^2 per data point. This regression used spherical, atom-centered interaction sites and did make the interaction between the C sp^2 and H sites more attractive than the C sp^3−H interaction, which seems consistent with the notion of additional π−H attraction. Further improvements were attempted using nonspherical C atoms. The C−C and C−H interactions were described with the product of two functions: one that describes the angular dependence and the other describes the distance dependency of the interaction energy. This approach did not produce as good a fit as an alternative method that we propose here. The π-electron clouds of the sp^2 C atoms were mimicked by placing four identical interaction sites (modified Morse functions, see eq 1) symmetrically above and below the C atoms.

The addition of these sites to the sp^2 C atoms improved the quality of fit to an SSR value of 0.039 (kcal/mol)^2 per alkene data point. This method is related to that proposed for modeling aromatic $\pi-\pi$ and H−π interactions of benzene by Hunter and Sanders,[29] but instead of point charges, Morse sites were used.

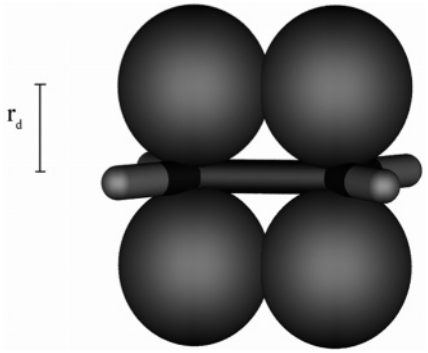

Figure 7. Ethylene with additional interaction centers. Two modified Morse functions are placed on ethylene to mimic the effects of π-electron clouds. Sites are symmetrically above and below the carbon nuclei (Morse site distance of r_d = 0.786 Å).

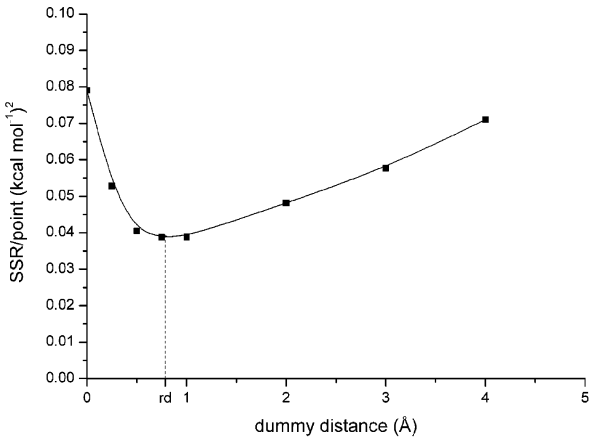

Figure 8. Sum of least-squares fitting error for alkene data as a function of additional Morse site distance (r_d) from sp^2 carbon. A minimum of 0.039 (kcal/mol)^2 per data point occurs at r_d = 0.7856 Å.

Morse sites do not restrict the interactions to being purely Coulombic or dispersive, because parameters were allowed to vary, to produce a best fit to alkene ab initio data. The auxiliary sites are positioned as shown in Figure 7, directly above and below each sp^2 C nucleus a distance r_d perpendicular to the CH_2=CH_2 plane. This has the intended effect of allowing atoms to approach more closely from the side and making the top approach more repulsive. This simple approach is easier to incorporate into standard molecular dynamics simulations than angular-dependent potentials and does not add significantly to computer processing unit (CPU) requirements. The optimum distance between the auxiliary sites and the sp^2 C nucleus was determined to be r_d = 0.7856 Å by performing a series of optimizations to the ab initio data for various values of r_d, in the range of 0−4 Å, as shown in Figure 8.

Parameter fitting was conducted with a simulated annealing global optimization algorithm by Goffe and other researchers; the details of the fitting algorithm can be found elsewhere.[38,43] This stochastic algorithm has been shown to be able to escape local minima of various fitting problems. Fourteen regression runs were conducted at a constant distance of r_d = 0.7856 Å, each starting from random initial guesses and search directions. Four of the runs converged to a secondary minimum with a larger SSR value; the remaining 10 runs converged to the same lower minimum, which we assume to be the global minimum. The original NIPE parameters were held constant for the appropriate alkyl interactions, to maintain transferability with alkanes; however, all other parameters were allowed to change in minimizing the total SSR. However, upper bounds (5.0 kcal/mol, 10.0 Å^{-1}, and 10.0 Å for ϵ, A, and r^*) and lower bounds

TABLE 5: Parameter Sets Describing the Alkene Data.

Best Fit of Alkene Data, Using Additional Interaction Sites				Parameter Sets, Using Spherical Atom-Centered Interaction Sites			
interaction, anisotropic carbons	ϵ (kcal/mol)	A (Å^{-1})	r^* (Å)	interaction, spherical atoms	ϵ (kcal/mol)	A (Å^{-1})	r^* (Å)
C3−C3[b]	0.05133	1.45985	4.34117	C1−C1	0.00260	1.06252	6.05150
C3−C2	0.32502	1.67319	3.57372	C1−C3	0.00009	1.21285	7.14454
C2−C2	1.31481	1.60410	3.22522	C3−C3[b]	0.05133	1.45985	4.34117
C3−H[b]	0.35562	2.11174	2.60211	C1−H	0.49423	1.83153	2.66136
C2−H	−0.02604	3.07464	2.63311	C3−H[b]	0.35562	2.11174	2.60211
H−H[b]	0.01048	1.26072	3.97536	H−H[b]	0.01048	1.26072	3.97536
C3-π	−0.03002	5.97642	2.49121				
C2-π	−0.01441	2.29966	3.11143				
H-π	0.00004	1.50785	5.04053				
$\pi-\pi$	0.00081	0.75152	6.89864				

[a] Two different cases are reported. The data on the left-hand side of the table are the best fit of alkene data, using additional interaction sites to mimic the π-electron clouds. The data on the right-hand side of the table are the parameter sets using spherical atom-centered interaction sites to describe the alkene data. The average squared residual is 0.039 (kcal/mol)^2 per data point for the anisotropic case and 0.085 (kcal/mol)^2 for the spherical atom case. [b] Fixed to previously reported NIPE parameters.[39]

(−0.04 kcal/mol, 0.0 Å^{-1}, 0.0 Å for ϵ, A, and r^*) were introduced to ensure that potentials would have appropriate repulsion ($\pi-\pi$) or dispersion behavior.

The anisotropic parameter set that produced the lowest SSR value is presented in Table 5. Also shown in Table 5 is the optimum parameter set when no auxiliary sites are used, or the spherical atom-centered case. The π-site interactions were determined to be repulsive, which is consistent with the benzene models.[29] Cross interactions of the π-sites with either carbon ($\pi-$C) or hydrogen ($\pi-$H) atoms are strongly attractive, as can be seen from Table 5. The minima for these pair attractions occur at fairly short distances. It seems that the minimum created by these attractions was missed by the four regression runs that did not find the global minimum.

We suspect that the origin of this attraction is strong electron correlation between approaching atoms and the high electron density in the π-bonds. The quality of the fit is significantly improved by the addition of the auxiliary π-sites, as seen by comparing the propene error maps in Figure 5, without (top) and with (bottom) auxiliary sites. Especially improved are the routes involving the *ae*-edge and the *abe*-face where the effect of the π-electrons would be most significant. The π-sites also substantially improved the ethylene interaction energy surface, an example of which is shown in Figure 6 where the original and anisotropic NIPE predictions are compared for the stacked-ethylene orientation.

5. Summary

Ethylene and propene dimer energy landscapes were investigated with ab initio methods. The ethylene D_{2d} dimer was determined to be the most favorable orientation. In the case of propene dimers, methyl groups were determined to interact strongly with the π-electron cloud, and the most-favorable orientations involved routes where sp^2-sp^3 carbon interactions were available. The interaction energy map generated in this work can be used as a starting point if the global minimum orientation of propene dimers is investigated. Attempts to predict the alkene interaction energy surfaces with the previously reported NIPE transferable potential model produced inaccuracies in orientations where the anisotropy of the sp^2 C atoms could be important. (NIPE is an acronym formed from the first letters of neopentane, isobutane, propane, and ethane.) The inclusion of anisotropy for the sp^2 C sites by the addition of auxiliary interaction sites directly above and below the carbon nucleus was determined to improve the description of ethylene and propene interaction energies significantly. This approach is simple and does not require major changes to simulation algorithms. In addition, for situations in which an anisotropy of atoms is not desired, a more-conventional but less-accurate parameter set (using spherical, atom-centered interaction sites) is also reported.

References and Notes

(1) Jalkanen, J.-P.; Pakkanen, T. A.; Rowley, R. L. *J. Chem. Phys.* **2004**, *120*, 1705.
(2) Allen, F. H.; Lommerse, J. P. M.; Hoy, V. J.; Howard, J. A. K.; Desiraju, G. R. *Acta Crystallogr., Sect. B: Struct. Sci.* **1996**, *B52*, 734.
(3) Hamilton, J. G.; Palke, W. E. *J. Am. Chem. Soc.* **1993**, *115*, 4159.
(4) Tsuzuki, S.; Tanabe, K. *J. Phys. Chem.* **1992**, *96*, 10804.
(5) Tsuzuki, S.; Uchimaru, T.; Tanabe, K. *Chem. Phys. Lett.* **1998**, *287*, 202.
(6) Brenner, V.; Millie, Ph. *Z. Phys. D* **1994**, *30*, 327.
(7) Tsuzuki, S.; Uchimaru, T.; Matsumura, K.; Mikami, M.; Tanabe, K. *Chem. Phys. Lett.* **2000**, *319*, 547.
(8) Tsuzuki, S.; Uchimaru, T.; Tanabe, K. *J. Mol. Struct. (THEOCHEM)* **1994**, *307*, 107.
(9) Tsuzuki, S.; Uchimaru, T.; Mikami, M.; Tanabe, K. *Chem. Phys. Lett.* **1996**, *252*, 206.
(10) Tsuzuki, S.; Uchimaru, T.; Mikami, M.; Tanabe, K. *J. Phys. Chem. A* **1998**, *102*, 2091.
(11) Tsuzuki, S.; Lüthi, H. P. *J. Chem. Phys.* **2001**, *114*, 3949.
(12) Tsuzuki, S.; Honda, K.; Uchimaru, T.; Mikami, M.; Tanabe, K. *J. Am. Chem. Soc.* **2000**, *122*, 3746.
(13) Špirko, V.; Engkvist, O.; Soldán, P.; Selzle, H. L.; Schlag, E. W.; Hobza, P. *J. Chem. Phys.* **1999**, *111*, 572.
(14) Hobza, P.; Selzle, H. L.; Schlag, E. W. *J. Am. Chem. Soc.* **1994**, *116*, 3500.
(15) Hobza, P.; Selzle, H. L.; Schlag, E. W. *J. Phys. Chem.* **1996**, *100*, 18790.
(16) Šponer, J.; Hobza, P. *Chem. Phys. Lett.* **1997**, *267*, 263.
(17) Hobza, P.; Selzle, H. L.; Schlag, E. W. *J. Chem. Phys.* **1990**, *93*, 5893.
(18) Hobza, P.; Selzle, H. L.; Schlag, E. W. *J. Phys. Chem.* **1993**, *97*, 3937.
(19) Gonzalez, C.; Lim, E. C. *J. Phys. Chem. A* **2000**, *104*, 2953.
(20) Tarakeshwar, P.; Choi, H. S.; Kim, K. S. *J. Am. Chem. Soc.* **2001**, *123*, 3323.
(21) Tarakeshwar, P.; Choi, H. S.; Lee, S. J.; Lee, J. Y.; Kim, K. S.; Ha, T.-K.; Jang, J. H.; Lee, J. G.; Lee, H. *J. Chem. Phys.* **1999**, *111*, 5838.
(22) Jaffe, R. L.; Smith, G. D. *J. Chem. Phys.* **1996**, *105*, 2780.
(23) Rozas, I.; Alkorta, I.; Elguero, J. *J. Phys. Chem. A* **1997**, *101*, 9457.
(24) Tsuzuki, S.; Honda, K.; Uchimaru, T.; Mikami, M.; Tanabe, K. *J. Am. Chem. Soc.* **2002**, *124*, 104.
(25) Tsuzuki, S.; Honda, K.; Uchimaru, T.; Mikami, M.; Tanabe, K. *J. Phys. Chem. A* **2002**, *106*, 4423.
(26) Tsuzuki, S.; Honda, K.; Azumi, R. *J. Am. Chem. Soc.* **2002**, *124*, 12200.
(27) Nishio, M.; Hirota, M.; Umezawa, Y. *The CH/π Interaction: Evidence, Nature, and Consequences*; Wiley−VCH: New York, 1998; p 55.
(28) Tsuzuki, S.; Honda, K.; Uchimaru, T.; Mikami, M.; Tanabe, K. *J. Phys. Chem. A* **1999**, *103*, 8265.
(29) Hunter, C. A.; Sanders, J. K. M. *J. Am. Chem. Soc.* **1990**, *112*, 5525.
(30) Tsuzuki, S.; Uchimaru, T.; Mikami, M.; Tanabe, K. *J. Phys. Chem. A* **2002**, *106*, 3867.

(31) Tsuzuki, S.; Tanabe, K. *J. Phys. Chem.* **1991**, *95*, 2272.
(32) Rappé, A. K.; Bernstein, E. R. *J. Phys. Chem. A* **2000**, *104*, 6117.
(33) Rowley, R. L.; Pakkanen, T. A. *J. Chem. Phys.* **1999**, *110*, 3368.
(34) Frisch, M. J.; Trucks, G. W.; Schlegel, H. B.; Scuseria, G. E.; Robb, M. A.; Cheeseman, J. R.; Zakrzewski, V. G.; Montgomery, J. A., Jr.; Stratmann, R. E.; Burant, J. C.; Dapprich, S.; Millam, J. M.; Daniels, A. D.; Kudin, K. N.; Strain, M. C.; Farkas, O.; Tomasi, J.; Barone, V.; Cossi, M.; Cammi, R.; Mennucci, B.; Pomelli, C.; Adamo, C.; Clifford, S.; Ochterski, J.; Petersson, G. A.; Ayala, P. Y.; Cui, Q.; Morokuma, K.; Malick, D. K.; Rabuck, A. D.; Raghavachari, K.; Foresman, J. B.; Cioslowski, J.; Ortiz, J. V.; Stefanov, B. B.; Liu, G.; Liashenko, A.; Piskorz, P.; Komaromi, I.; Gomperts, R.; Martin, R. L.; Fox, D. J.; Keith, T.; Al-Laham, M. A.; Peng, C. Y.; Nanayakkara, A.; Gonzalez, C.; Challacombe, M.; Gill, P. M. W.; Johnson, B. G.; Chen, W.; Wong, M. W.; Andres, J. L.; Head-Gordon, M.; Replogle, E. S.; Pople, J. A. *Gaussian 98*, revision A.9; Gaussian, Inc.: Pittsburgh, PA, 1998.
(35) Boys, S. F.; Bernardi, F. *Mol. Phys.* **1970**, *19*, 553.
(36) Lochmann, R.; Weller, T. *J. Mol. Struct. (THEOCHEM)* **1983**, *104*, 91.
(37) Rowley, R. L.; Yang, Y.; Pakkanen, T. A. *J. Chem. Phys.* **2001**, *114*, 6058.
(38) Jalkanen, J.-P.; Mahlanen, R.; Pakkanen, T. A.; Rowley, R. L. *J. Chem. Phys.* **2002**, *116*, 1303.
(39) Jalkanen, J.-P.; Pakkanen, T. A.; Yang, Y.; Rowley, R. L. *J. Chem. Phys.* **2003**, *118*, 5474.
(40) Blowers, P.; Masel, R. I. *J. Phys. Chem. A* **1999**, *103*, 7725.
(41) Hart, J. R.; Rappé, A. K. *J. Chem. Phys.* **1992**, *97*, 1109.
(42) Hart, J. R.; Rappé, A. K. *J. Chem. Phys.* **1993**, *98*, 2492.
(43) Goffe, W. L.; Ferrier, G. D.; Rogers, J. *J. Econometrics* **1994**, *60*, 65.